ISSN 0915-633X

NATIONAL INSTITUTE FOR FUSION SCIENCE

An Accurate Nonlinear Monte Carlo Collision Operator

W.X. Wang, M. Okamoto, N. Nakajima and S. Murakami

(Received - Feb. 14, 1995)

NIFS-345 Mar. 1995

RESEARCH REPORT
NIFS Series

NAGOYA, JAPAN

An Accurate Nonlinear Monte Carlo Collision Operator

W. X. Wang[†], M. Okamoto[†,‡], N. Nakajima [†,‡], and S. Murakami[†,‡]

[†]Department of Fusion Science, The Graduate University for Advanced Studies,

Nagoya 464-01, Japan

[‡]Theory and Data Analysis Division, National Institute for Fusion Science,

Nagoya 464-01, Japan

Abstract

A three dimensional nonlinear Monte Carlo collision model is developed based on Coulomb binary collisions with the emphasis both on the accuracy and implementation efficiency. The operator of simple form fulfills particle number, momentum and energy conservation laws, and is equivalent to exact Fokker-Planck operator by correctly reproducing the friction coefficient and diffusion tensor, in addition, can effectively assure small-angle collisions with a binary scattering angle distributed in a limited range near zero. Two highly vectorizable algorithms are designed for its fast implementation. Various test simulations regarding relaxation processes, electrical conductivity, etc. are carried out in velocity space. The test results, which is in good agreement with theory, and timing results on vector computers show that it is practically applicable. The operator may be used for accurately simulating collisional transport problems in magnetized and unmagnetized plasmas.

Keywords: Coulomb binary collision, Fokker-Planck collision operator, Monte Carlo collision operator, vector calculation.

1 Introduction

Collisional transport is a fundamental aspect of the physics of magnetically confined plasmas. Neoclassical theory of transport, which has well developed, is valid under two essential assumptions, namely $\rho_p \ll L_T, L_n$, and $M_p \ll 1$, where ρ_p is poloidal Larmor radius, L_T, L_n are scale lengths of plasma temperature and density respectively, and M_p is poloidal Mach number. In the edge region of toroidal systems, the situations with $\rho_p \geq L_T, L_n$ and $M_p \geq 1$ are often observed(e.g. H-mode). In this case, standard neoclassical theory can not be applied. Monte Carlo simulation[1-3] may provide a powerful way for solving the problems. We are developing a Monte Carlo simulation code for the purpose of studying neoclassical transport near edge. The Monte Carlo method can be briefly summarized as follows. The simulation region is divided into a lot of spatial cells such that plasma in each cell can be considered to be uniform. Initially, particles are distributed randomly in cells and velocity space in terms of given plasma conditions such as density profile and temperature profile. The drift motion of each particle is then followed in magnetic coordinate in which MHD equilibrium is employed. In the process of following particle drift motion, Coulomb binary collisions are introduced by an appropriate Monte Carlo operator. Finally, the transport properties of interest are evaluated in terms of relevant information.

Constructing an appropriate Monte Carlo collision operator is an essential step in the simulation. The investigations of Monte Carlo operator have been motivated by studies of many interested processes involving collisions in plasma physics, for example. plasma heating[4-6] in torus and gyrokinetic simulation[7-9], et al. There are some efforts addressed to this topic for different purpose. Shanny et al.[10], to the purpose of electron plasma simulation, and Boozer and Kuo-Petravic[1], to the purpose of collisional transport in stellarator , introduced respectively the Monte Carlo operators based on Lorentz gas collision model which describes electron-ion collisions. To model the effect of ion-ion collisions on ion-temperature-gradients modes, Xu and Resenbluth[11] constructed a linear Monte Carlo scheme, combined with gyrokinetic particle simulation model. Monte Carlo operator for orbit-averaged Fokker-Planck equation was given by Eriksson and Hellender[6], and White et al.[12]. The application of such linear operators is limited due to, fundamentally, lack of momentum conservation. The momentum conservation, as required by exact Fokker-Planck collision operator, is necessary condition for ambipolarity of par-

ticle fluxes, and therefore, is essential in many cases for correct simulation. for example, in the calculations of plasma flow(rotation) and bootstrap current. Recent development in this topic relates with gyrokinetic plasma simulation. The Monte Carlo operator for δf particle simulation[9,13-15] has been proposed by Dimits and Cohen[16], in which energy and momentum conservations are approximately restored by the introduction of sink/source terms in the gyrokinectic equation. Based on the discretization of linearized Fokker-Planck gyrokinetic equation, Tassarotto, White and Zheng[17,18] constructed the linear Monte Carlo operators with fulfillment of momentum and energy conservations through including momentum and energy restoring terms in it. However, its numerical implementation is not straightforward and convenient because of the complicated forms and tedious calculation for restoring terms. A nonlinear Monte Carlo collision operator of PIC model was proposed earlier by Takizuka and Abe[19], and extended to gyrokinetics simulation by Ma, Sydora and Dawson[20]. In this model, the scattering angle of a binary collision obeys a Gaussian distribution, and large-angle deflection is not effectively avoided when the step size for the collision integral is not sufficient small. The overestimate of large-angle collisions may lead to the simulation results inconsistent with the Fokker-Planck equation[20].

In this paper, an accurate 3D nonlinear Monte Carlo operator is developed , which is simple in form and easy for numerical implementation. The basic features of the operator are that it fulfills all basic conservation laws, namely, momentum, energy and particle number conservations, which are characteristic of exact Fokker-Planck operator; it is equivalent to the exact collision operator of Landau form; moreover, the small-angle collision characteristic is effectively assured by distributing the scattering angle in a small range near zero. As a consequence, the basic collisional transport properties can be correctly described, for example, in particular, strict ambipolarity of particle fluxes is obtained automatically. The final feature mentioned above is helpful to release the limitation on integral step size, compared to previous nonlinear operator[19,20]. Noting that collision calculation is very time-consuming, we pay much attention to its fast implementation in vector computer, and design two vectorizable algorithms, which as an important component part, make the operator directly applicable.

The paper is organized as follows. First the Monte Carlo operator is presented in its original form. The procedure of construction of the operator is given in order to

demonstrate the properties of the operator. Then, we address to its fast numerical implementation, and present two vectorizable algorithms of practical application. After that, the operator is tested carefully in velocity space. The tests include relaxation processes and electric conductivity, etc. The conclusions are summarized finally.

2 Monte Carlo Collision Operator

A general useful Monte Carlo operator should satisfy two-fold requirement. Physically, it is applicable to the problem to be solved. Generally speaking, it fulfill all basic conservation laws, i.e, conserves particle number, momentum, and energy. Strictly, sometimes it needs to be equivalent to exact Fokker-Planck operator for accurate simulation. Numerically, it is feasible and is convenient for its implementation. In particular, its computational cost in time and memory is acceptable by current computer.

Here, first we present the Monte Carlo operator in its original form, which indeed satisfy the requirement in physics mentioned above. The Monte Carlo operator is constructed for the Coulomb binary collisions in local space, a spatial cell with uniform plasma. Without loss of generality, simple plasma system (electrons plus one species ions) is employed for the convenience of presentation. Consider a spatial cell with electron density n_e and ion density n_i, correspondingly, the model system with N_e electrons and N_i ions. We here impose a condition $N_e/n_e = N_i/n_i$, which is the representation, in model system, of plasma neutrality. For a neutral plasma close to thermodynamic equilibrium, the Coulomb collision interaction between particles is within the distance of order λ_D due to Debye shielding, where λ_D is Debye radius. Thus, a typical size of a cell is the Debye radius. In many cases, however, one can extend the cell size in terms that plasma properties across each cell does not vary substantially.

Let that each particle collides with all other particles at same cell in time interval Δt. When considering collisions, the particle positions in a cell are trivial and not concerned. In practice, Monte Carlo operator gives the particle random kicks in velocity space with appropriate magnitudes and directions. The velocity alteration of particle a$(m_a, \vec{v_a}, e_a)$ during a collision with particle b$(m_b, \vec{v_b}, e_b)$ in a time interval Δt is determined as follows,

$$\Delta\vec{v_a} = \frac{m_b}{m_a + m_b}(e^{\epsilon\hat{n}\times} - 1)\vec{u}, \tag{1}$$

and small parameter ϵ is given by

$$\frac{\epsilon^2 u^3}{3} = \Delta t(4\pi e_a^2 e_b^2 \ln\Lambda)(\frac{1}{m_a} + \frac{1}{m_b})^2\gamma, \tag{2}$$

where, for different type of collisions,

$$\gamma = \begin{cases} n_b/N_b = n_a/N_a, & \text{unlike} - \text{particle collisions} \\ n_a/(N_a - 1), & \text{like} - \text{particle collisions} \end{cases},$$

$\vec{u} = \vec{v_a} - \vec{v_b}$ is the relative velocity before the collision, $\ln\Lambda$ is Coulomb logarithm, and $\hat{n}$ is a random unit vector with uniform distribution. In the implementation, the operation $(e^{\epsilon\hat{n}\times} - 1)$ is performed through following approximate expansion,

$$e^{\epsilon\hat{n}\times} - 1 = \sin\epsilon\hat{n}\times + (1 - \cos\epsilon)\hat{n}\times\hat{n}\times . \tag{3}$$

$\epsilon \ll 1$ gives restriction to step size Δt of collision integration.

Next, we shall explain how to construct the Monte Carlo operator and demonstrate the properties of the operator. Consider Coulomb collision of two model particles a and b in three-dimension, as shown in Fig.1a. There are six quantities (the velocity components of two particles) that can change during collision. However, energy conservation and momentum conservation impose four constraints. Thus, only two parameters can freely change. These two free parameters correspond to usually impact parameter ρ(or scattering angle θ) and azimuthal angle ϕ shown in Fig.1b. The fact that there are two free choices implies that there are two random variables included in a 3D Monte Carlo operator. In Takizuka and Abe's model[19], they are selected to be direction angles Θ and Φ of the postcollision relative velocity $\vec{u}'$ in terms of precollision relative velocity $\vec{u}$ (Fig.1c). Here, two random variables are combined and selected to be a random unit vector $\hat{n}$ of uniform distribution.

With momentum conservation

$$m_a\vec{v_a} + m_b\vec{v_b} = m_a\vec{v_a}' + m_b\vec{v_b}', \tag{4}$$

energy conservation requires that the magnitude of relative velocity does not change during the collision, i.e,

$$\mid \vec{u}' \mid = \mid \vec{u} \mid . \tag{5}$$

Then, set the postcollision relative velocity as

$$\vec{u}' = \tilde{R}\vec{u} = [e^{\epsilon\hat{n}\times}]\vec{u}, \tag{6}$$

where ϵ is a infinitesimal and nondimensional parameter to be determined later. It is readily to show that $\vec{u}'$ satisfies Eq.(5). From Eq.(4) and (6) we obtain Eq.(1), which, through $\hat{n}$ and ϵ, determines the change of the velocity after a collision. In practical implementation, the use of approximation (3) does not violate Eq.(5), and therefore does not violate energy conservation.

The remaining task is to determine ϵ. ϵ is determined in terms of the requirement that the Monte Carlo operator expressed by Eq.(1) and (3) is equivalent to exact Fokker-Planck operator

$$C_{ab} = -\frac{\partial}{\partial \vec{v}}[\frac{<\Delta\vec{v}>}{\Delta t} f_a] + \frac{1}{2}\frac{\partial}{\partial \vec{v}}\frac{\partial}{\partial \vec{v}} : [\frac{<\Delta\vec{v}\Delta\vec{v}>}{\Delta t} f_a], \tag{7}$$

where $<\Delta\vec{v}>/\Delta t$ and $<\Delta\vec{v}\Delta\vec{v}>/\Delta t$ are friction coefficient and diffusion tensor respectively. To this purpose, we calculate the corresponding coefficients of the Monte Carlo operator as follows (if $b = a$, $N_b \to N_a - 1$ in the calculation),

$$\begin{aligned} <\Delta\vec{v}>_{M.C} &\equiv <\sum_{j=1}^{N_b}\Delta\vec{v}_j>_{\hat{n}} \\ &= -\sum_{j=1}^{N_b}\frac{m_b}{m_a+m_b}\frac{\epsilon^2 u_j^3}{3}\frac{\vec{u}_j}{u_j^3} + O(\epsilon^4), \end{aligned} \tag{8}$$

$$\begin{aligned} <\Delta\vec{v}\Delta\vec{v}>_{M.C} &\equiv <\sum_{i=1}^{N_b}\Delta\vec{v}_i\sum_{j=1}^{N_b}\Delta\vec{v}_j>_{\hat{n}} \\ &= \sum_{j=1}^{N_b}<\Delta\vec{v}_j\Delta\vec{v}_j>_{\hat{n}} + O(\epsilon^4) \\ &= \sum_{j=1}^{N_b}(\frac{m_b}{m_a+m_b})^2\frac{\epsilon^2 u_j^3}{3}\frac{u_j^2\overleftrightarrow{I} - \vec{u}_j\vec{u}_j}{u_j^3} + O(\epsilon^4), \end{aligned} \tag{9}$$

where

$$<\Delta\vec{v}_j>_{\hat{n}} \equiv \frac{1}{4\pi}\int\Delta\vec{v}_j d\Omega, \quad \text{and} \quad <\Delta\vec{v}_j\Delta\vec{v}_j>_{\hat{n}} \equiv \frac{1}{4\pi}\int\Delta\vec{v}_j\Delta\vec{v}_j d\Omega.$$

We expect that the Monte Carlo operator can correctly reproduce friction coefficient and diffusion tensor. Compared to the analytical coefficients, it is found that the quantity $\epsilon^2 u_j^3/3$ in Eq.(8) and (9) should be set as

$$\frac{\epsilon^2 u_j^3}{3} = \Delta t(4\pi e_a^2 e_b^2 \ln\Lambda)(\frac{1}{m_a} + \frac{1}{m_b})^2\frac{n_b}{N_b}. \tag{10}$$

Assuming that model particles are sufficient to form a velocity correctly distributed local background, the summations can accurately reproduce the average over background distribution $f_b(\vec{v})$,

$$\sum_{j=1}^{N_b} \longrightarrow \frac{N_b}{n_b} \int d\vec{v}' f_b(\vec{v}'). \tag{11}$$

Thus, as $\Delta t \to 0$, the Monte Carlo operator can give exact friction coefficient and diffusion tensor,

$$\lim_{\Delta t \to 0} \frac{<\Delta \vec{v}>_{M.C}}{\Delta t} = -\frac{4\pi e_a^2 e_b^2 \ln \Lambda}{m_a} \int d\vec{v}' f_b(\vec{v}') \frac{\vec{u}}{u^3} (\frac{1}{m_a} + \frac{1}{m_b}), \tag{12}$$

$$\lim_{\Delta t \to 0} \frac{<\Delta \vec{v} \Delta \vec{v}>_{M.C}}{\Delta t} = \frac{4\pi e_a^2 e_b^2 \ln \Lambda}{m_a} \int d\vec{v}' f_b(\vec{v}') \frac{u^2 \overleftrightarrow{I} - \vec{u}\vec{u}}{u^3} \frac{1}{m_a}. \tag{13}$$

To make the operator more physically understandable, we give an insight into the relation between random unit vector $\hat{n}$ and Θ and Φ. Set $\vec{u}$ along $\hat{z}$ direction (Fig.1c). In the Cartesian coordinate random unit vector can be expressed as

$$\hat{n} = \sin\theta \cos\varphi \hat{x} + \sin\theta \sin\varphi \hat{y} + \cos\theta \hat{z} \tag{14}$$

with $\cos\theta$ uniformly taking random value between -1 and 1, and φ uniformly taking random value between 0 and 2π. Then from the operator, we obtain

$$\cos\Theta = \frac{\vec{u} \cdot \vec{u}'}{u^2} = 1 - (1 - \cos\epsilon)\sin^2\theta, \tag{15}$$

$$\tan\Phi = \frac{u_y'}{u_x'} = \tan(\varphi - \alpha) \tag{16}$$

with $\cot\alpha \equiv \cos\theta \tan(\epsilon/2)$. From Eq.(15) we have $0 \leq \Theta \leq \epsilon$. Hence, when $\epsilon \ll 1$ the operator always gives small-angle scattering, which is consistent with Fokker-Planck operator. With having Eg.(16), we can readily prove that Φ can take any value between 0 and 2π with equal probability. This point reflects the fact that $\vec{u}'$ (or $\Delta\vec{u}$) is isotropic in the direction perpendicular to $\vec{u}$.

It is place to point out the signaficant difference between the model here and that of Takizuka and Abe[19]. It is well known that in a plasma small-angle collisions are much important than collisions resulting in large momentum changes, and the large-angle deflections mainly result from accumulation of multiple small-angle collisions. In fact, Fokker-Planck operator describes the effect on distribution function resulting from frequently occurring small-angle collisions. In Takizuka and Abe's model, scattering angle Θ is determined through sampling $\tan(\Theta/2)$ according to a Gaussian distribution. Even

though the variance of the Gaussian distribution is small (small variance is also required to reproduce correct friction coefficient and diffusion tensor), there are still some probabilities for Θ taking large value, therefore, as noted in [20], to keep consistency with Fokker-Planck operator, step size should be small enough to ensure that the majority of collisions are small-angle. In the present model, as mentioned above, if ϵ is small, large angle scattering never occurs. In this sense, the operator here is more reasonable to approach Fokker-Planck problem. In other words, it may allow one to use large step size to increase calculation efficiency.

Different from Θ in Takizuka and Abe's model, the random parameter $\hat{n}$ is independent of quantities of binary particles and other simulation parameters. This feature may bring us some convenience in the implementation.

3 Fast Implementation — Algorithms Suitable for Vector Calculation

The Monte Carlo operator presented in last section is simple in form, and its implementation is straightforward and convenient. We here remark one point about the implementation.

Coulomb collisions in a plasma, as we know, are simultaneous interaction. i.e, one particle may simultaneously experience the forces exerted by a number of particles around it, due to the character of long-range interaction. In the Monte Carlo model, however, a particle velocity changes step by step in time interval Δt as it collides with other particles one by one. The one-by-one collisions may affect the long time statistical properties of the system. Determining collision order in an optimal way is essential in the model. Obviously, determining collision order in a completely random way may greatest reduce this effect. One simple way to determine collision order is shown in Fig.2. First, all particles in a cell are randomly arranged in a line. The particle with index $I(1)$ collides with all other particles behind it first, then does the particle with index $I(2)$, and so on. Although the determination of collision order by above way is not completely random, the examinations show that it is effective to give satisfactory results, in addition, fewer calculation for sorting is needed in this way.

Monte Carlo calculation of collisions is very time consuming. The computational time

cost for a cell is proportional to N^2, where N is the total particle number in the cell. To reduce statistical error, large number of particles are needed in each cell. In addition, to apply it in practical simulation evolving configuration space, a lot of cells are needed to reflect the spatial variety of a plasma. Thus, its fast implementation with high efficiency is essential for it to be practically applicable. Vector calculation provides a very effective way for the speedup. Unfortunately, the operator in its original form is not suitable for the vector implementation. We next present two vectorizable algorithms.

Algorithm 1 .

The implementation of the original operator in each time interval Δt consists of three steps: generating uniform random unit vector, arranging collision order and calculating the changes of particle velocities, among which the final step contains most of floating-point calculation and is most time-consuming. In each time interval Δt, one particle collides with all other particles in the same cell, and its velocity changes many times. This gives rise to the difficulty to vectorize the final step. The difficulty also relates to second step—how to arrange collision order.

Now imagine that the time interval Δt is divided into many small time intervals Δt_i. At each small time interval Δt_i, particles in the same cell are paired in a random way for collisions. We expect that, in time interval Δt, each particles may pair all other particles in the same cell. This is an alternate way to reproduce the average over the background distribution. We next explain the details.

To pair particles for collisions, we use the same method as in Takizuka and Abe's model[19]. At first, the particles of same species are randomly arranged in lines. Then, pairing particles is performed as follows. Like particles are paired as shown in Fig.3. If particle number is even, particles are paired in order from the top of the line(Fig.3a). If particle number is odd, the first three particles are paired in three pairs(Fig.3b). Unlike particles are paired as shown in Fig.4. When $N_e = N_i$, electrons and ions are paired in order from the top of the lines(Fig.4a). If $N_e \neq N_i$, for example $N_e > N_i$ ($N_e/Ni = i + r$, where i is a positive integer and $0 \leq r < 1$), electrons and ions are divided into two groups, first group with $(i+1)rN_i$ electrons and rN_i ions, and second group with $i(1-r)N_i$ electrons and $(1-r)N_i$ ions. Each ion of the first is selected $i+1$ times to pair an electron of the first, and each ion of the second is selected i times to pair an electron of the second (Fig.4b).

Having done pairing particles and generating $\hat{n}$(the latter is easily vectorized), we calculate the velocity change after a collision by Eq.(1) and (3) . However, Eq.(2). used for giving small parameter ϵ, is here modified,

$$\frac{\epsilon^2 u^3}{3} = \Delta t_i (4\pi e_a^2 e_b^2 \ln \Lambda)(\frac{1}{m_a} + \frac{1}{m_b})^2 \gamma, \tag{17}$$

and for different cases,

$$\gamma = \begin{cases} n_a/2. & \text{for first three like} - \text{particle collisions when } N_a = \text{odd}, \\ n_L \equiv \min(n_a, n_b), & \text{otherwise.} \end{cases}$$

With the way of pairlike collisions, the calculations of velocity changes can be vectorized now. We can understand that the modified operator, as the original one, is equivalent to exact Fokker-Planck collision operator with following two observations: 1. determining collision pairs by above way means sampling v_b (or v_a) in $\vec{u} \equiv \vec{v_a} - \vec{v_b}$ according to background distribution $f_b(\vec{v})$ (or $f_a(\vec{v})$); 2. in Fig.4a, the probabilities of a electron (or a ion) being in the first group and the second group are, respectively. $(i+1)rN_i/N_e = (i+1)r/(r+1)$ (or $rN_i/N_i = r$) and $i(1-r)N_i/N_e = i(1-r)/(i+r)$ (or $(1-r)N_i/N_i = 1-r$).

Algorithm 2 .

We note that algorithms 1 is effective when $N_e = N_i$ =even, and, however, it is complicated in logic in other cases, especially when $N_e = odd \neq N_i$ =odd. In general case, its implementation is not so convenient, and more essentially, the complexity in logic may give rise to additional computational cost. In practice, the particle numbers in a cell is not fixed, and the cases without $N_e = N_i = even$ are often met. The algorithm 2, as to be seen next, is more practically applicable in the sense that it is universally effective to handle general case.

For the convenience of presentation, an example with 7 electrons and 6 ions is employed here. At first, as in algorithm 1, electrons (and ions) in a cell are randomly arranged in a line (Fig.5a). In a step of time interval Δt, for unlike-particle collisions, let one electron collides with all ions in the same cell. The ergodic unlike-particle collisions are performed by the way of "round robin", as shown in Fig.5b (where the final electron in each round draws a bye). For like-particle collisions, we divide electrons (and ions) into two groups, group A with $N_{eA} = int(N_e/2)$ (=3 for our example) electrons and group B with $N_{eB} = int[(N_a+1)/2]$ (=4 for our example) electrons, as shown in Fig.5a. and let one

particle in a group collides with all particles in another group. The like-particle collisions between the two groups are then performed by the same way as in unlike-particle collisions (Fig.5c).

The velocity change after a collision is calculated by Eq.(1), (2), and by Eq.(3) in which, for like-particle collisions of species a, the factor γ is modified as

$$\gamma = \frac{n_a}{2(N_{cn}/N_a)},$$

where $N_{cn} \equiv N_{aA}N_{aB}$ is the like-particle collision number of species a in time interval Δt.

Note that particles that belong to same group do not collide each other in a time step. If necessary, we can immediately improve this point by further dividing a group into two subgroups. The particle collisions between two subgroups are performed by the same way as shown in Fig.5c without additional difficulty. Correspondingly, the factor γ given above changes as the like-particle collision number N_{cn} changes.

The algorithm presented here is highly vectorizable thanks to the way that particles are grouped for collisions.

4 Test

The Monte Carlo operator should be tested carefully in order to be applied. To this purpose, we have simulated various problems in velocity space concerning relaxation processes, derivation from Maxwellian distribution and electrical conductivity. For simplicity, a simple plasma system with $n_e = n_i$, thus $N_e = N_i$ and charge number $Z = 1$ is employed in the simulations.

(1) Relaxation between electron temperature T_e and ion temperature T_i .

In the simulation, set initially electrons and ions are both Maxwellian, but with different temperatures $T_e \neq T_i$. Due to Coulomb collisions, electrons and ions will relax to equilibrium, and T_e and T_i will approach to same temperature. This process is described by

$$\frac{dT_e}{dt} = \frac{T_i - T_e}{\tau_T^{e/i}}, \tag{18}$$

$$n_e T_e + n_i T_i = n_e T_{e0} + n_i T_{i0}, \tag{19}$$

where

$$\tau_T^{e/i} = \frac{1}{2\sqrt{2}}(\frac{T_e}{T_{e0}} + \frac{m_e}{m_i}\frac{T_i}{T_{e0}})^{3/2}\tau_0$$

with the relaxation time defined as

$$\tau_0 = \frac{m_i}{m_e}\frac{3\sqrt{m_e}}{4\sqrt{\pi}e_e^2 e_i^2 n_i \ln\Lambda}T_{e0}^{3/2}.$$

The result of a simulation by using the original operator with $N_e = N_i = 400$ and $T_{e0}/T_{i0} = 2$ is shown in Fig.6, in which the Monte Carlo operator gives good agreement with theory.

(2) Relaxation between longitudinal temperature $T_\parallel$ and transverse temperature $T_\perp$.

Now we consider the thermal isotropization process in a single species particle system in which the particles are initially in the distribution

$$f_{a0} = n_a(\frac{m_a}{2\pi T_{\parallel 0}})^{1/2}(\frac{m_a}{2\pi T_{\perp 0}})\exp(-\frac{m_a}{2T_{\parallel 0}}v_{\parallel 0}^2 - \frac{m_a}{2T_{\perp 0}}v_{\perp 0}^2)$$

with $T_{\parallel 0} \neq T_{\perp 0}$. In theory, following equations can describe the relaxation between $T_\parallel$ and $T_\perp$

$$\frac{dT_\perp}{dt} = -\frac{1}{2}\frac{dT_\parallel}{dt} = -\frac{T_\perp - T_\parallel}{\tau_T^a}, \tag{20}$$

where

$$\tau_T^a = \frac{2}{3}(\frac{T_\parallel}{T_{a0}})^{3/2}A^2\tau_a \begin{cases} [-3 + (A+3)\frac{\tan^{-1}\sqrt{A}}{\sqrt{A}}]^{-1}, & A > 1 \\ [-3 + (A+3)\frac{\tanh^{-1}\sqrt{-A}}{\sqrt{-A}}]^{-1}, & A < 1 \end{cases},$$

with the relaxation time here defined as

$$\tau_a = \frac{3\sqrt{m_a}}{4\sqrt{\pi}e_a^4 n_a \ln\Lambda}T_{a0}^{3/2},$$

$T_{a0} = (2T_{\perp 0} + T_{\parallel 0})/3$ and $A = T_\perp/T_\parallel - 1$.

This process is modeled by the Monte Carlo operator. The time evolutions of difference between $T_\parallel$ and $T_\perp$ are illustrated in Fig.7 with $N_e = 2000$, $T_{\parallel 0} = 1.5keV$ and $T_{\perp 0} = 2.5keV$. Here the original operator is used. The good agreement between the Monte Carlo results and analytical result is obtained under different time step sizes (Δt in Fig.7b is 4 times that in Fig.7a).

(3) Derivation from the isotropic distribution .

As a test of the accuracy of the operator, a system with 1000 initially Maxwellian particles is observed in time to see its derivation from the isotropic distribution. The observation is shown in Fig.8, from which we can conclude two points: the fluctuations of three temperatures T_x, T_y and T_z are within 5%, and the derivation from the isotropic distribution does not increase with time.

(4) Electrical conductivity .

The next test is regarding parallel electrical conductivity. Set initially electrons and ions are in equilibrium. A magnetic field and an electric field are introduced along $\hat{z}$ direction. Due to different electrical accelerations, the relative motion between electrons as a whole and ions as a whole occurs in $\hat{z}$ direction, and as the result, a current $j_{\|}$ along $\hat{z}$ direction is created. Meanwhile, due to ohmic heating electron temperature increases. In this case, since system is not in steady state, the simple Ohm's law $j_{\|} = \sigma_{\|} E$ is not valid, where $\sigma_{\|}$ denotes parallel electrical conductivity. Instead, following equations can describe the problems,

$$\frac{3}{2} n_e \frac{dT_e}{dt} = \frac{j_{\|}^2}{\sigma_{\|}} - 3\sqrt{2} n_e (\frac{T_{e0}}{T_e})^{3/2} \frac{T_e - T_i}{\tau_0}, \tag{21}$$

$$\frac{3}{2} n_i \frac{dT_i}{dt} = 3\sqrt{2} n_e (\frac{T_{e0}}{T_e})^{3/2} \frac{T_e - T_i}{\tau_0}, \tag{22}$$

$$\frac{dV_e}{dt} = -\frac{e}{m_e} E + \frac{e}{m_e} \frac{j_{\|}}{\sigma_{\|}}, \tag{23}$$

$$\frac{dV_i}{dt} = \frac{e}{m_i} E - \frac{e}{m_i} \frac{n_e}{n_i} \frac{j_{\|}}{\sigma_{\|}}, \tag{24}$$

$$j_{\|} = -e n_e (V_e - V_i). \tag{25}$$

We solve Eq.(18)–(22) by Runge Kutta method to obtain the analytical result. When we solve the equations, the theoretical parallel electrical conductivity

$$\sigma_{\|} = 1.96 \frac{3 T_e^{3/2}}{4\sqrt{2\pi} \ln \Lambda e^2 \sqrt{m_e}} \tag{26}$$

is used.

The Monte Carlo result obtained by algorithm 1 with $N_e = N_i = 1000$, $B = 0.1T$ and $E = 0.2 E_d$ (E_d denotes Dreicer field), as well as the analytical result are shown in Fig.9, in which T_e and $j_{\|}$ are plotted versus t/τ_e. We can see that the Monte Carlo result agrees well

with the theory. In addition, a series of simulations with different parameters have been carried out, and shown that the Monte Carlo operator can correctly give the dependences of $\sigma_{\parallel}$ expressed in Eq.(23), i.e, the numerical factor is about 1.96, $\sigma_{\parallel}$ is proportional to $T_e^{3/2}$ and is independent of B, E, and plasma densities.

(5) Relaxation of initially shifted Maxwellian distribution .

We again use a system of 1000 electrons and 1000 ions, and employ algorithm 1. Initially, electrons are in a shifted Maxwellian distribution

$$f_{e0} = n_e(\frac{m_e}{2\pi T_{e0}})^{3/2} \exp[-\frac{m_e}{2T_{e0}}(\vec{v} - \vec{V}_{e0})^2],$$

and ions are Maxwellian with $T_{i0} = T_{e0}$. At first stage, collisional dissipation transfers electron kinetic energy to thermal energy and leads electron to reach equilibrium. The temperature T_e and current j evolutions given by the Monte Carlo simulation with $\frac{1}{2}m_e V_{e0}^2/T_{e0} = 1.09$ are shown in Fig.10, as the comparison, also shown analytical result which is obtained by Eq.(18)–(22) with electric field $E = 0$.

We here remark that the three operators (original one, algorithm 1 and algorithm 2), all can give the correct results for above tests. In VPX vector computer, for one of above tests, the vector implementation by using algorithm 1 for the case of $N_e = N_i$=even, is 4-5 times faster than the scalar implementation by using the original operator. However, the vector implementation by using algorithm 2 always gives such high efficiency in general, not only the case of $N_e = N_i$=even, but also other cases. The CPU cost for the calculation of one collision in SX-3 supercomputer is about 1.5×10^{-7} second. As the comparison, the Monte Carlo results obtained by algorithm 2 are illustrated in Fig.11, which is regarding the equilibration of T_e and T_i, and the thermal isotropization between $T_{\parallel}$ and $T_{\perp}$.

5 Conclusions

A 3D Monte Carlo collision model based on Coulomb binary collision has been developed with the emphasis both on the accuracy and the implementation efficiency.

The exact momentum conservation and energy conservation fulfilled by the operator are assured through the consideration of elastic binary collisions. Since the operator is constructed in a spatial cell, the conservations are local. The accurate Monte Carlo operator is equivalent to the exact Fokker-Planck operator by correctly reproducing the friction

coefficient and diffusion tensor through the leading order. The small-angle scattering characteristic can be effectively assured in the model by small parameter ϵ.

The implementation is straightforward and convenient due to its simple form. For the practical application, the vectorizable algorithms have been designed. A high efficiency for speedup has been achieved in vector computer. The point that the scattering angle of a binary collision is restrained to be small may allow one to enlarge step size for collision integral, and therefore to increase the implementation efficiency. The timing results on VPX vector computer and SX-3 supercomputer show that the computational cost is acceptable to use it in some practical simulations (we are using it in a Monte Carlo simulation code to study egde neoclassical transport).

The relaxation processes, electrical conductivity and Ohmic heating in uniform plasmas have been simulated as the test of the model. The Monte Carlo results show good agreement with theory.

The present Monte Carlo operator show some advantages compared to earlier approximate operators (the linear operators) some of which do not fulfill basic conservation laws. As noticed before[15], the violation of conservation laws may result in incorrect result in the simulations of some problems. The operator constructed in general case, is widely useful for different problems in both magnetized and unmagnetized plasmas because it makes fewer assumptions. Its nonlinear form makes it more applicable for accurate simulation. In principle, it is potentially useful for general nonlinear problems involving the evolution of distribution functions far from equilibrium, where the previous linear operators can not be applied. Such an important example is electron transport process in laser produced plasmas. The model can be readily extended for the use in particle simulation and gyrokinetic simulation.

Compared to Takizuka and Abe's model[19], in which the scattering angle of a binary collision is determined in terms of a Gaussian distribution, and thus, to reduce the probability for occurring large angle deflection, the sufficient small step size is needed to get the consistent results with the theory[20], the present model may be more efficient to approach Fokker-Planck problems since the scattering is limited within a small ϵ. In addition, the fast implementation in vector computer is achieved by two vectorizable algorithms, in particular algorithm 2, which make present operator directly applicable.

ACKNOWLEDGEMENTS

The authors would like to thank Dr. R.Kanno for useful discussions during the preparation of the paper. One of the authors (Wang) wishes to acknowledge the hospitality of the Theory and Data Analysis Division of National Institute for Fusion Science. He would like to thank Prof. Tieqiang Chang for the continuous encouragement. He is supported by the Japanese Ministry of Education, Science and Culture (MONBUSHO).

References

[1] A. H. Boozer and G. Kuo-Petravic, Phys. Fluids **24**, 851(1981).

[2] R. H. Fowler, J. A. Rome and J. F. Lyon, Phys. Fluids **28**, 338(1985).

[3] W. Lotz, and J. Nührenberg, Phys. Fluids **31**. 2984(1988).

[4] S. Murakami, M. Okamoto, N. Nakajima, M. Ohnish and H. Okada, Nucl. Fusion **34**, 913(1994).

[5] M. A. Kovanen, W. G. F. Core and T. Hellsten, Nucl. Fusion **32**, 787(1992).

[6] L.-G. Eriksson and P. Helander, Phy. Plasmas **1**, 308(1994).

[7] W. W. Lee, J. Comput. Phys. **72**, 243(1987).

[8] T. Tajima, *Computational Plasma Physics* (Addison-Wesley, Redwood City, CA, 1989).

[9] A. M. Dimits and W. W. Lee, J. Comput. Phys. **107**, 309(1993).

[10] R. Shanny, J. M. Dawson and J. H. Greene, Phys. Fluids **10**, 1281(1967).

[11] X. Q. Xu and M. N. Rosenbluth, Phys. Fluids **B 3**, 627(1991).

[12] R. B. White, A. H. Boozer, R. Goldston, H. Hay, J. Albert, and C. F. F. Karey, in *Plasma Physics and Controlled Nuclear Fusion Research* (International Atomic Energy Agency, Vienna, 1982) Vol.3, p. 391.

[13] M. Kotchenreuther, Bull. AM. Phys. Soc. **34**, 2107(1988).

[14] G. DiPeso E. C. Morse and R. W. Ziolkowki, J. Comput. Phys. **96**, 325(1991).

[15] M. Tessarotto, R. B. White and L. J. Zheng, Phy. Plasmas **1**, 2603(1994).

[16] A. M. Dimits and B. I. Cohen, Phys. Rev. E **49**, 709(1994).

[17] M. Tessarotto, R. B. White and L. J. Zheng, Phy. Plasmas **1**, 951(1994).

[18] M. Tessarotto, R. B. White and L. J. Zheng, Phy. Plasmas **1**, 2591(1994).

[19] T. Takizuka and H. Abe, J. Comput. Phys. **25**, 205(1977).

[20] S. Ma, R. D. Sydora and J. M. Dawson, Comput. Phys. Commun. **77**, 190(1993).

Figure Captions

Fig. 1 A sketch of Coulomb binary collision.

Fig. 2 Determination of collision order.

Fig. 3 After index randomization, like-particles are paired for binary collisions. Particle number (a) N =even, and (b) N =odd.

Fig. 4 Electrons and ions are paired for collisions. (a) $N_e = N_i$. (b) $N_e > N_i$.

Fig. 5 Particles are grouped for collisions (an example of 7 electrons and 6 ions). (a) Electrons (and ions) are randomly arranged in a line and divided into Group A and B, (b) i-e collisions are performed by the way of "round robin" where in each round the final electron draws a bye. (c) Like-particle collisions between Group A and B are performed by the same way.

Fig. 6 Temporal relaxation between electron temperature T_e and ion temperature T_i (by original operator).

Fig. 7 Temporal relaxation between longitudinal temperature $T_\parallel$ and perpendicular temperature $T_\perp$ (by original operator).

Fig. 8 Deviation from isotropic distribution.

Fig. 9 The results of a test regarding parallel electrical conductivity (by Algorithm 1). Time evolution of (a) electron temperature T_e due to Ohmic heating, and (b) parallel current $j_\parallel$.

Fig. 10 Relaxation of initially shifted Maxwellian distribution (by Algorithm 1). (a) Electron temperature T_e versus t/τ_e. (b) Current j versus t/τ_e.

Fig. 11 Thermal relaxation processes simulated by using Algorithm 2. (a) Temporal relaxation between T_e and T_i with $T_e/T_i = 2$ and $N_e = N_i = 513$. (a) Temporal relaxation between $T_\parallel$ and $T_\perp$ with $T_\perp/T_\parallel = 2$ and $N_e = 2111$.

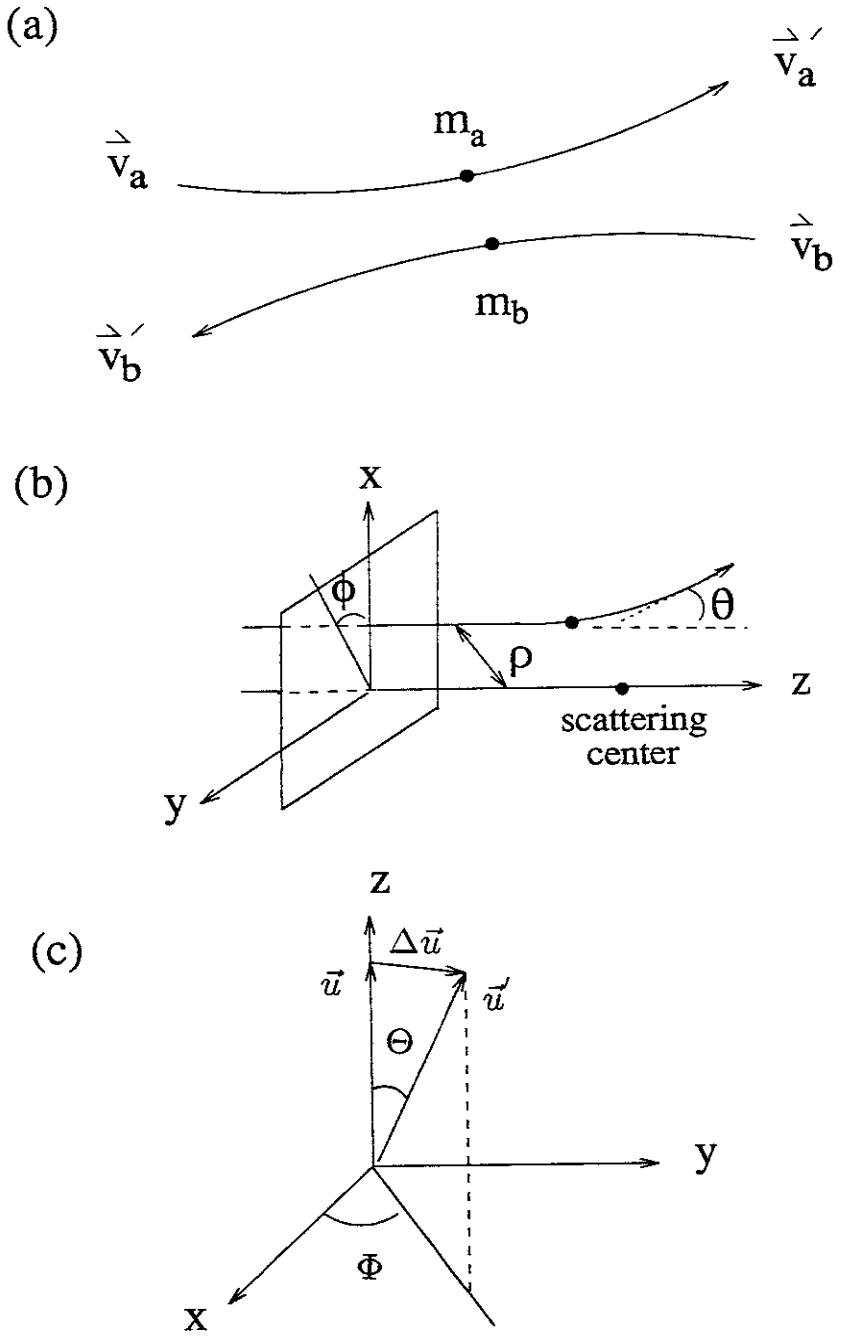
(a)
$\vec{v}_a'$
m_a
$\vec{v}_a$
$\vec{v}_b$
m_b
$\vec{v}_b'$
(b)
x
ϕ
θ
ρ
z
scattering
center
y
(c)
z
$\Delta\vec{u}$
$\vec{u}$
$\vec{u}'$
Θ
y
Φ
x

Fig. 1

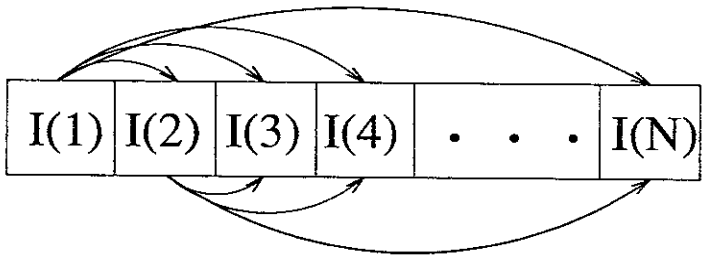

Fig. 2

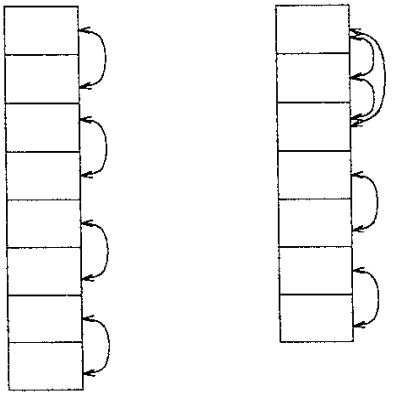

(a) N =even (b) N =odd

Fig. 3

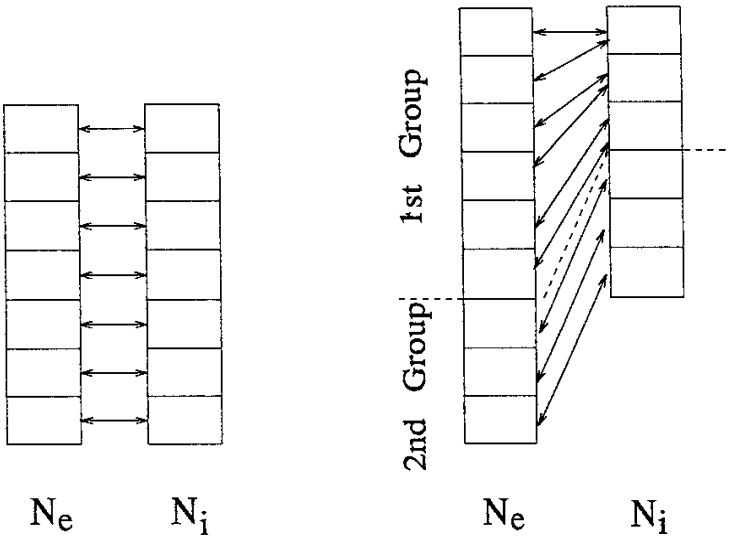

(a) $N_e = N_i$ (b) $N_e > N_i$

Fig. 4

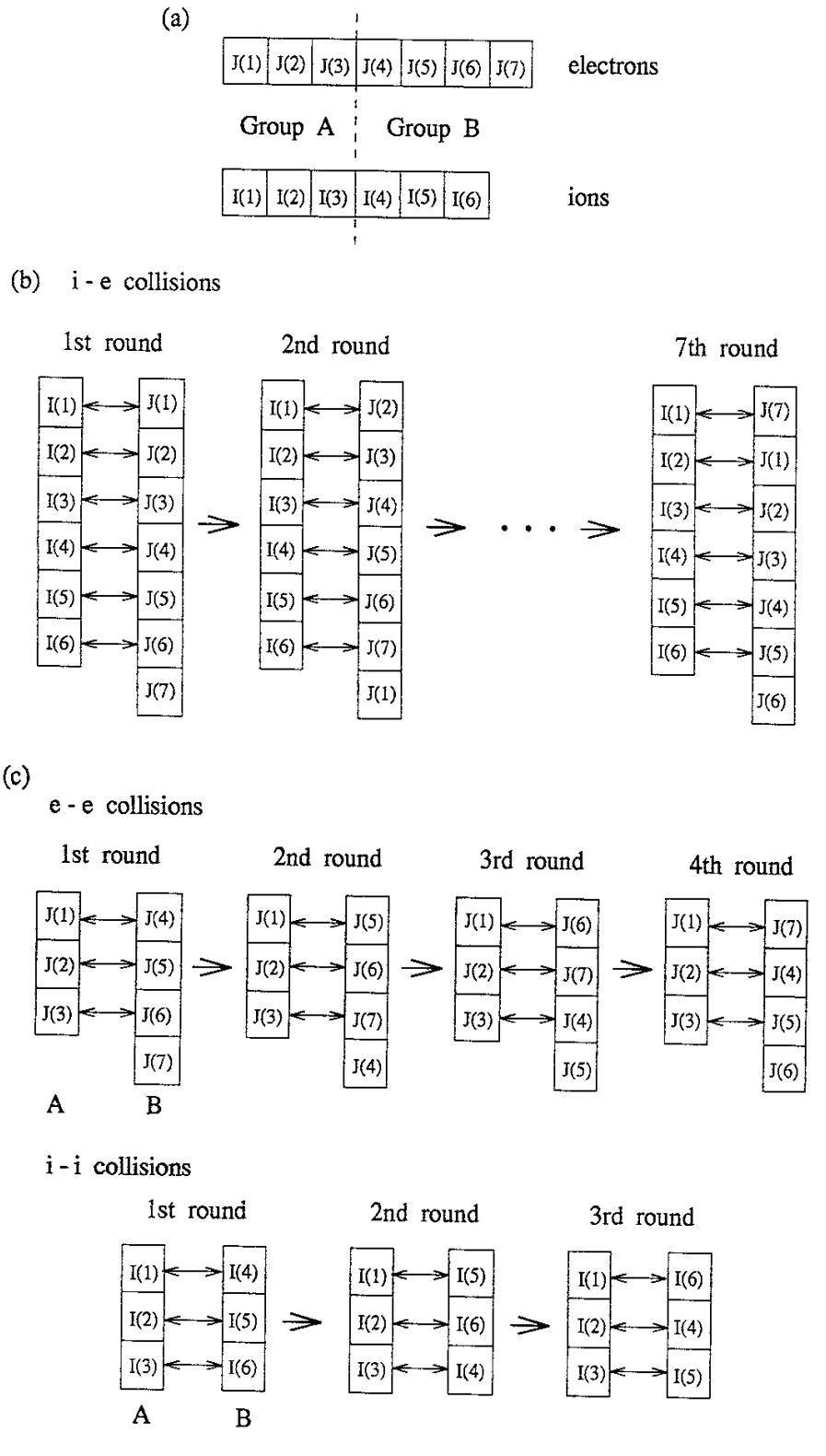
(a)
J(1) J(2) J(3) J(4) J(5) J(6) J(7)
electrons
Group A
Group B
I(1) I(2) I(3) I(4) I(5) I(6)
ions
(b) i - e collisions
1st round
2nd round
7th round
(c)
e - e collisions
1st round
2nd round
3rd round
4th round
A
B
i - i collisions
1st round
2nd round
3rd round
A
B

Fig. 5

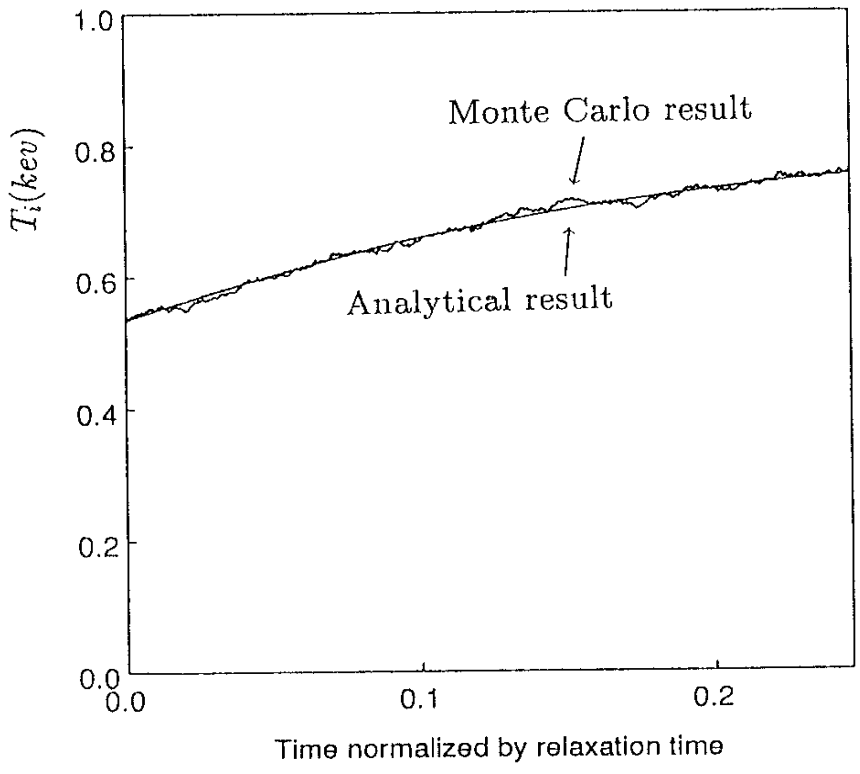
$T_i(kev)$
1.0
0.8
0.6
0.4
0.2
0.0
0.0
0.1
0.2
Monte Carlo result
Analytical result
Time normalized by relaxation time

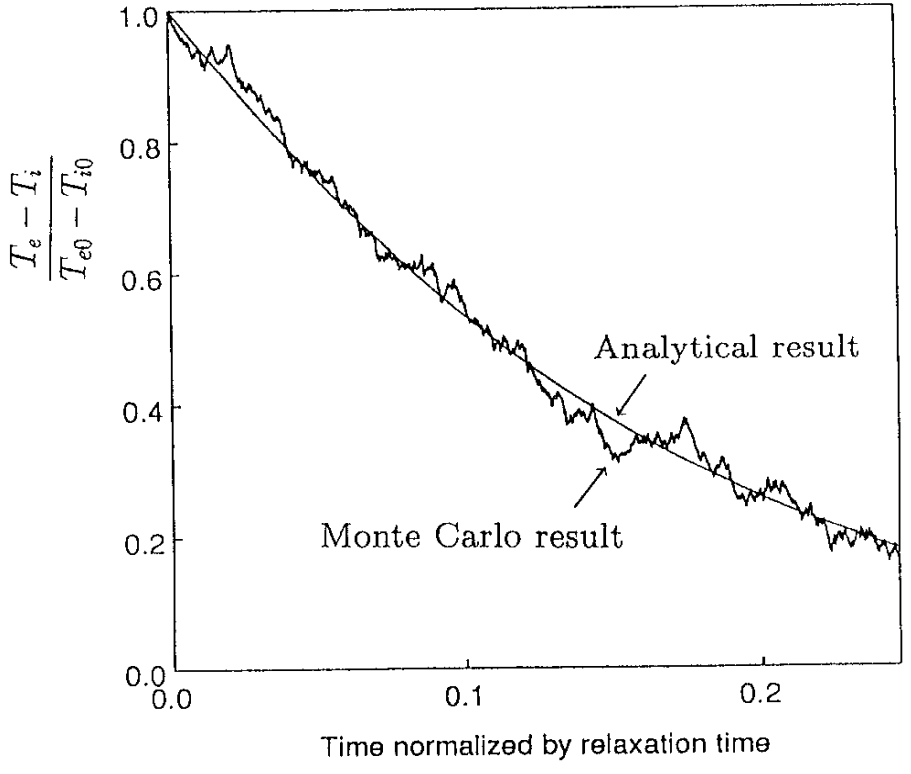
$\frac{T_e - T_i}{T_{e0} - T_{i0}}$
1.0
0.8
0.6
0.4
0.2
0.0
0.0
0.1
0.2
Analytical result
Monte Carlo result
Time normalized by relaxation time

Fig. 6

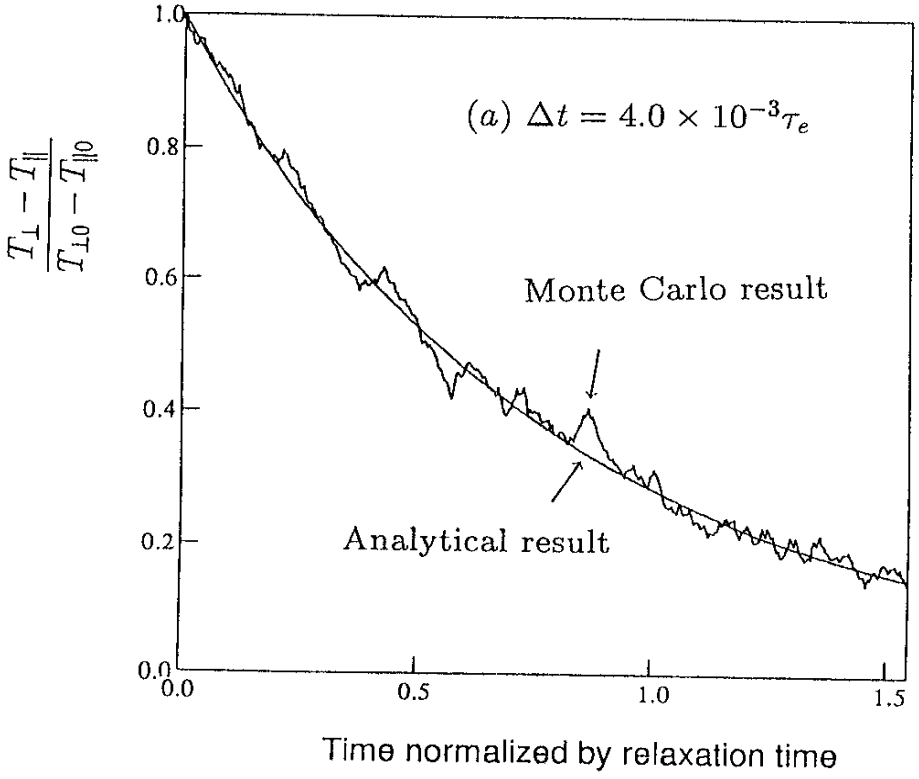
$\frac{T_\perp - T_\parallel}{T_{\perp 0} - T_{\parallel 0}}$
1.0
0.8
0.6
0.4
0.2
0.0
0.0
0.5
1.0
1.5
$(a)\ \Delta t = 4.0 \times 10^{-3}\tau_e$
Monte Carlo result
Analytical result
Time normalized by relaxation time

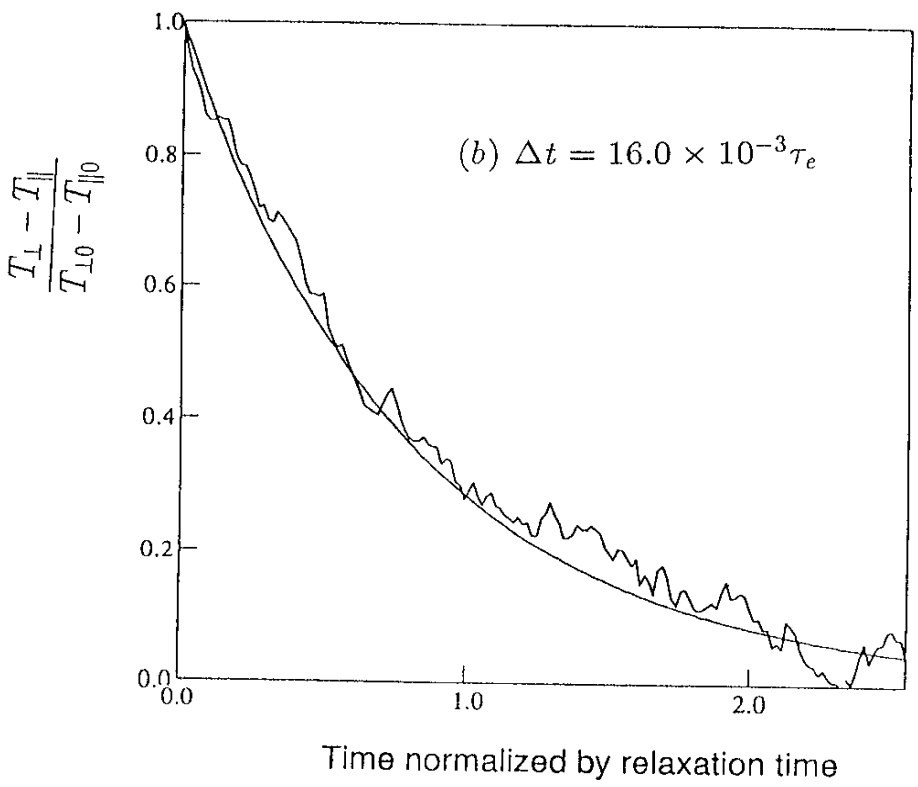
$\frac{T_\perp - T_\parallel}{T_{\perp 0} - T_{\parallel 0}}$
1.0
0.8
0.6
0.4
0.2
0.0
0.0
1.0
2.0
$(b)\ \Delta t = 16.0 \times 10^{-3}\tau_e$
Time normalized by relaxation time

Fig. 7

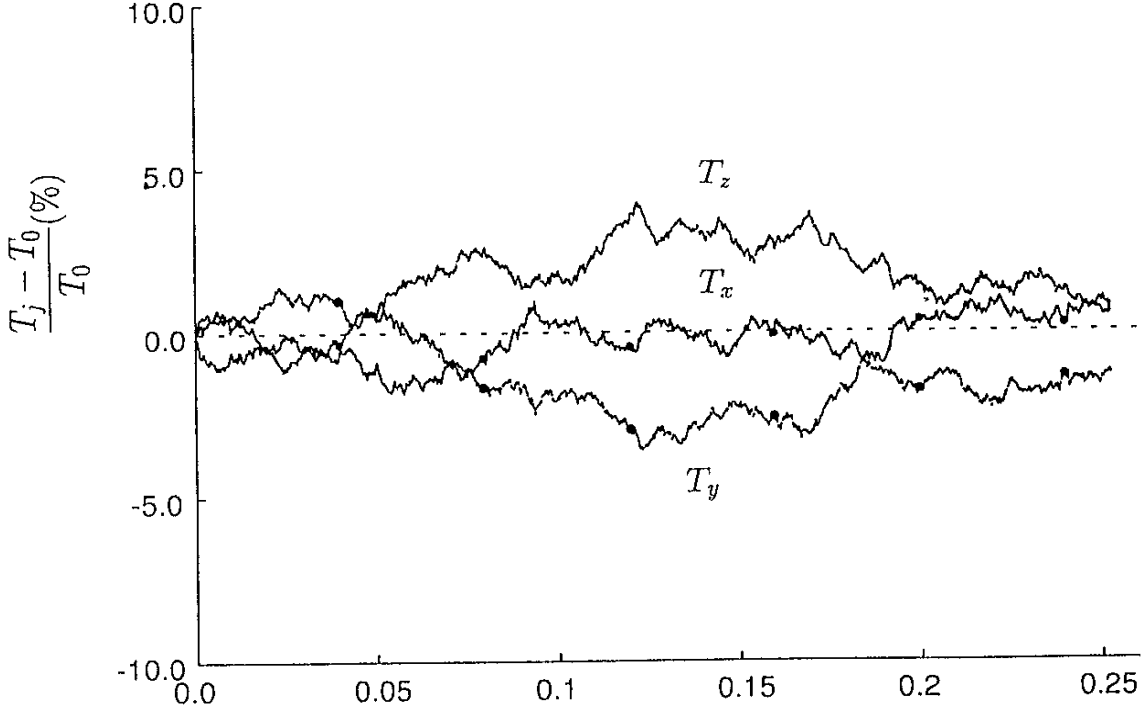
10.0
5.0
0.0
-5.0
-10.0
0.0
0.05
0.1
0.15
0.2
0.25
T_z
T_x
T_y
$\frac{T_j - T_0}{T_0}(\%)$
Time normalized by rexalation time

Fig. 8

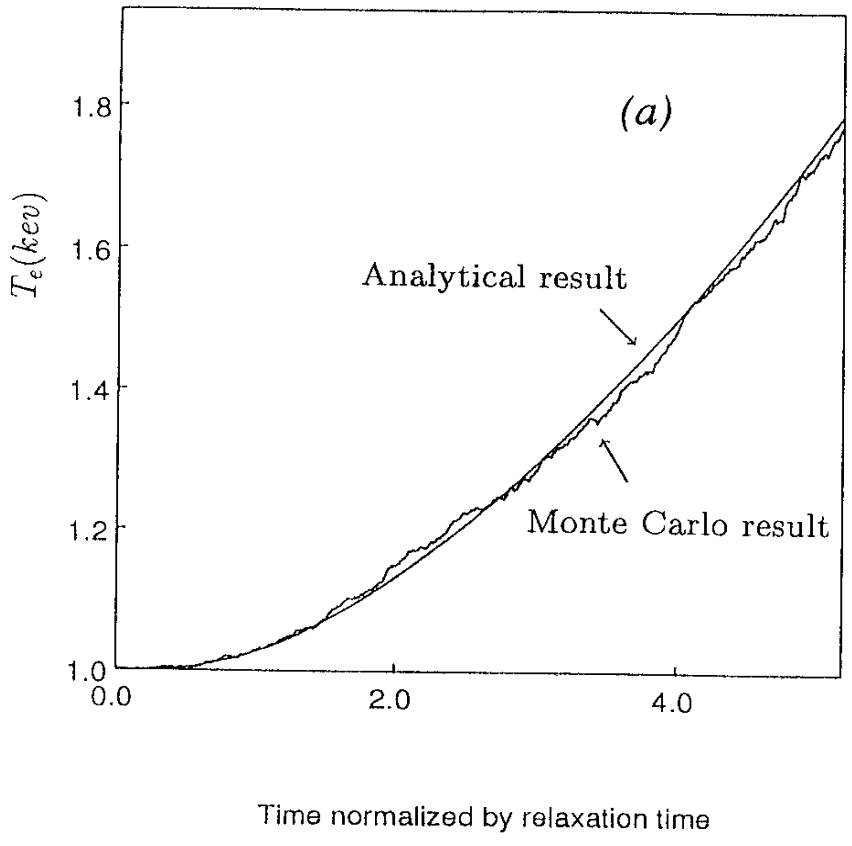
(a)
$T_e(kev)$
1.8
1.6
1.4
1.2
1.0
0.0
2.0
4.0
Analytical result
Monte Carlo result
Time normalized by relaxation time

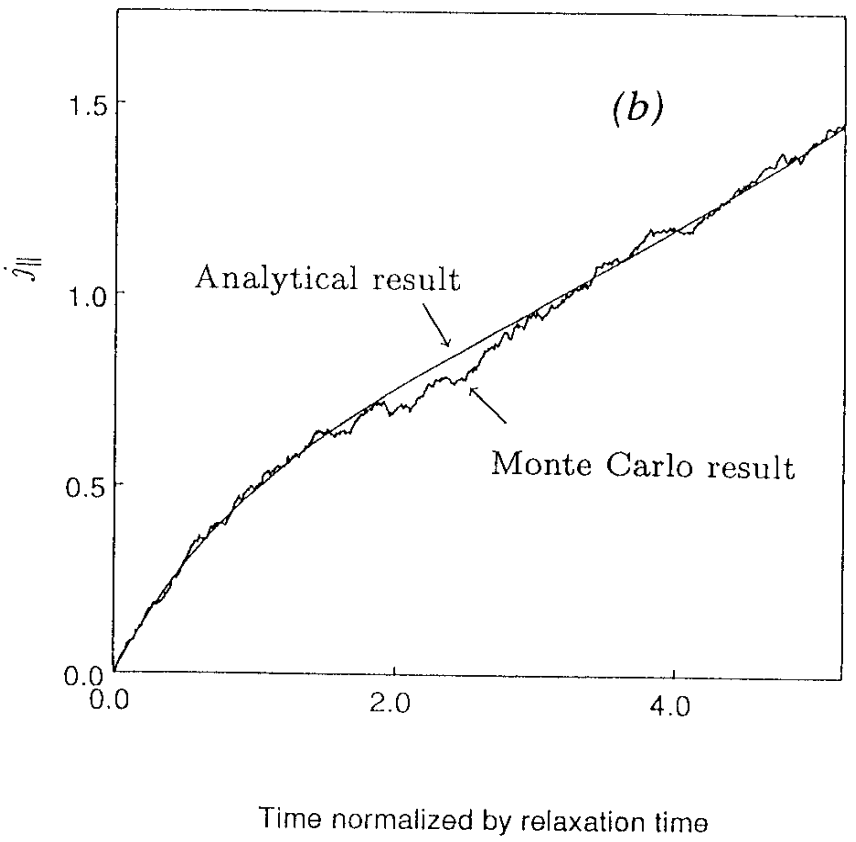
(b)
$j_{\parallel}$
1.5
1.0
0.5
0.0
0.0
2.0
4.0
Analytical result
Monte Carlo result
Time normalized by relaxation time

Fig. 9

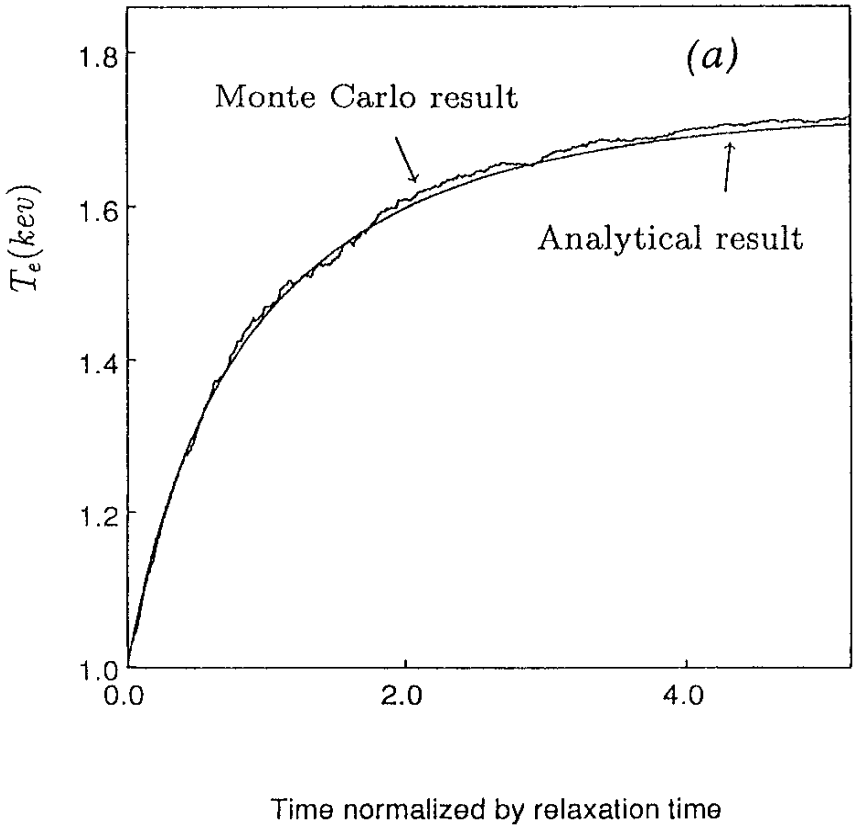
(a)
Monte Carlo result
Analytical result
$T_e(kev)$
1.8
1.6
1.4
1.2
1.0
0.0
2.0
4.0
Time normalized by relaxation time

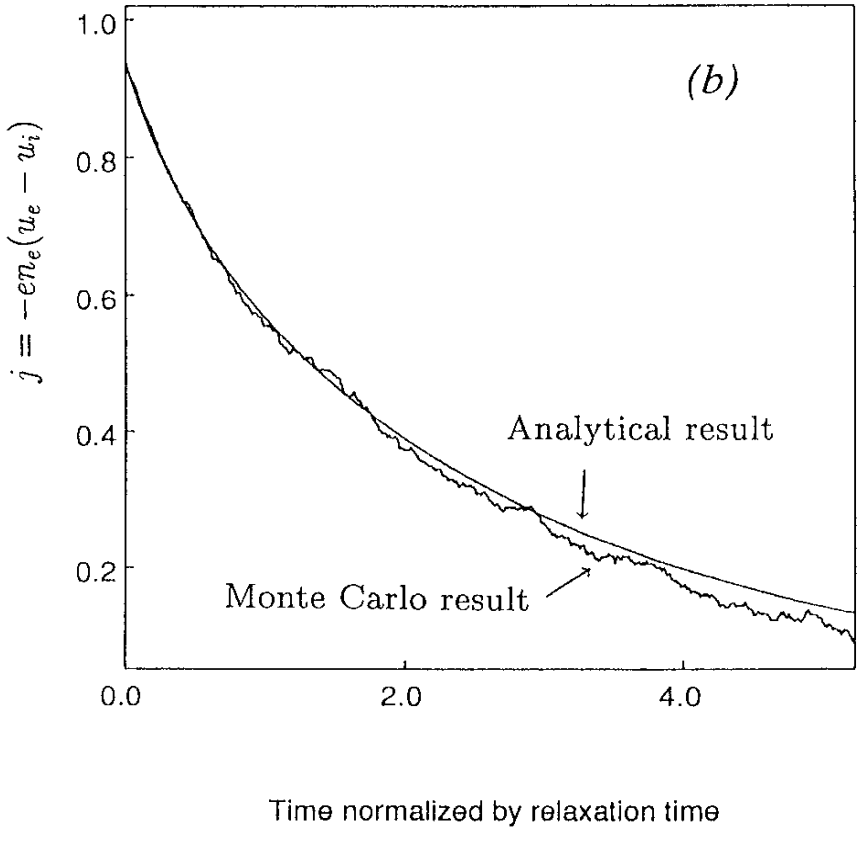
(b)
Analytical result
Monte Carlo result
$j = -en_e(u_e - u_i)$
1.0
0.8
0.6
0.4
0.2
0.0
2.0
4.0
Time normalized by relaxation time

Fig. 10

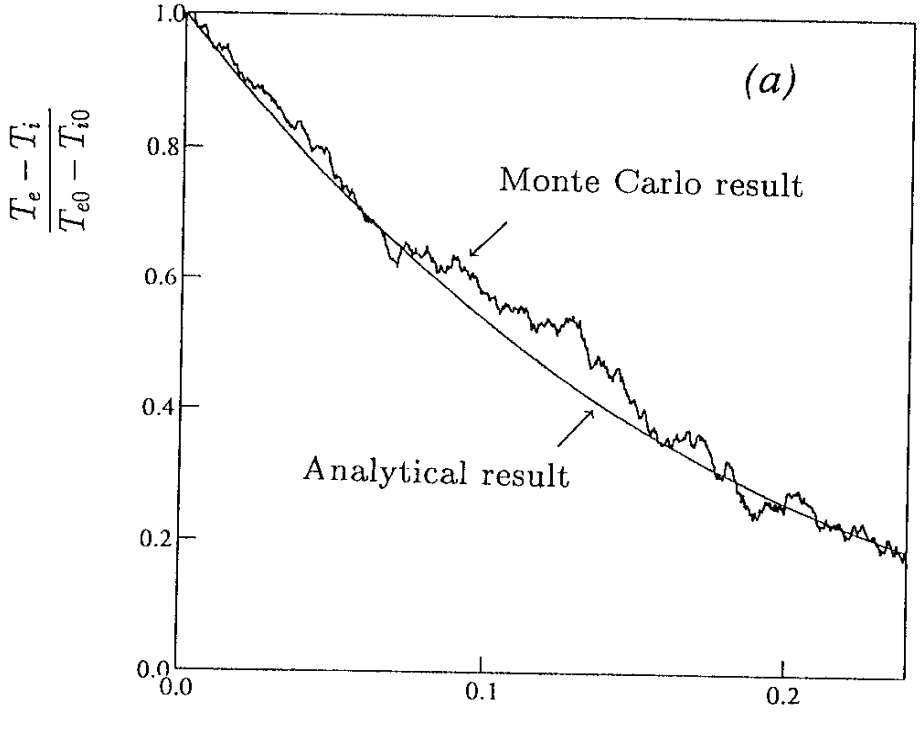
$\frac{T_e - T_i}{T_{e0} - T_{i0}}$
1.0
0.8
0.6
0.4
0.2
0.0
0.0
0.1
0.2
(a)
Monte Carlo result
Analytical result
Time normalized by rexalation time

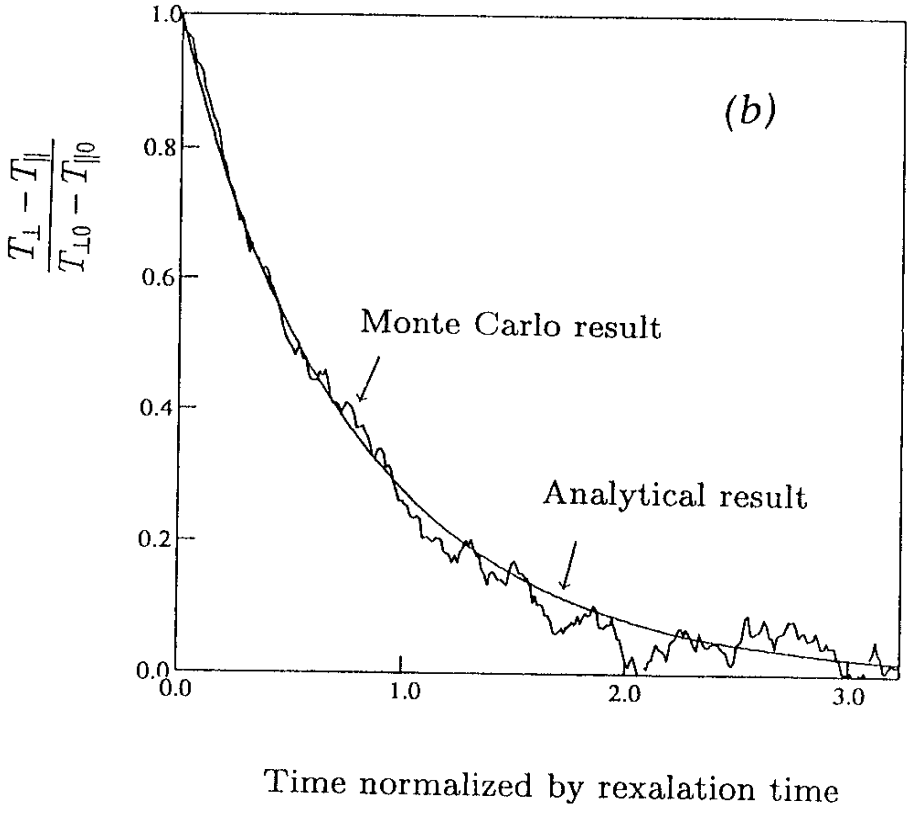
$\frac{T_\perp - T_\parallel}{T_{\perp 0} - T_{\parallel 0}}$
1.0
0.8
0.6
0.4
0.2
0.0
0.0
1.0
2.0
3.0
(b)
Monte Carlo result
Analytical result
Time normalized by rexalation time

Fig. 11

Recent Issues of NIFS Series

NIFS-301 Y. Hamada, A. Nishizawa, Y. Kawasumi, K.N. Sato, H. Sakakita, R. Liang, K. Kawahata, A. Ejiri, K. Narihara, K. Sato, T. Seki, K. Toi, K. Itoh, H. Iguchi, A. Fujisawa, K. Adachi, S. Hidekuma, S. Hirokura, K. Ida, M. Kojima, J. Koog, R. Kumazawa, H. Kuramoto, T. Minami, I. Negi, S. Ohdachi, M. Sasao, T. Tsuzuki, J. Xu, I. Yamada, T. Watari, *Study of Turbulence and Plasma Potential in JIPP T-IIU Tokamak*; Aug. 1994 (IAEA/CN-60/A-2-III-5)

NIFS-302 K. Nishimura, R. Kumazawa, T. Mutoh, T. Watari, T. Seki, A. Ando, S. Masuda, F. Shinpo, S. Murakami, S. Okamura, H. Yamada, K. Matsuoka, S. Morita, T. Ozaki, K. Ida, H. Iguchi, I. Yamada, A. Ejiri, H. Idei, S. Muto, K. Tanaka, J. Xu, R. Akiyama, H. Arimoto, M. Isobe, M. Iwase, O. Kaneko, S. Kubo, T. Kawamoto, A. Lazaros, T. Morisaki, S. Sakakibara, Y. Takita, C. Takahashi and K. Tsumori, *ICRF Heating in CHS*; Sep. 1994 (IAEA-CN-60/A-6-I-4)

NIFS-303 S. Okamura, K. Matsuoka, K. Nishimura, K. Tsumori, R. Akiyama, S. Sakakibara, H. Yamada, S. Morita, T. Morisaki, N. Nakajima, K. Tanaka, J. Xu, K. Ida, H. Iguchi, A. Lazaros, T. Ozaki, H. Arimoto, A. Ejiri, M. Fujiwara, H. Idei, A. Iiyoshi, O, Kaneko, K. Kawahata, T. Kawamoto, S. Kubo, T. Kuroda, O. Motojima, V.D. Pustovitov, A. Sagara, C. Takahashi, K. Toi and I. Yamada, *High Beta Experiments in CHS*; Sep. 1994 (IAEA-CN-60/A-2-IV-3)

NIFS-304 K. Ida, H. Idei, H. Sanuki, K. Itoh, J. Xu, S. Hidekuma, K. Kondo, A. Sahara, H. Zushi, S.-I. Itoh, A. Fukuyama, K. Adati, R. Akiyama, S. Bessho, A. Ejiri, A. Fujisawa, M. Fujiwara, Y. Hamada, S. Hirokura, H. Iguchi, O. Kaneko, K. Kawahata, Y. Kawasumi, M. Kojima, S. Kubo, H. Kuramoto, A. Lazaros, R. Liang, K. Matsuoka, T. Minami, T. Mizuuchi, T. Morisaki, S. Morita, K. Nagasaki, K. Narihara, K. Nishimura, A. Nishizawa, T. Obiki, H. Okada, S. Okamura, T. Ozaki, S. Sakakibara, H. Sakakita, A. Sagara, F. Sano, M. Sasao, K. Sato, K.N. Sato, T. Saeki, S. Sudo, C. Takahashi, K. Tanaka, K. Tsumori, H.Yamada, I. Yamada, Y. Takita, T. Tuzuki, K. Toi and T. Watari, *Control of Radial Electric Field in Torus Plasma;* Sep. 1994 (IAEA-CN-60/A-2-IV-2)

NIFS-305 T. Hayashi, T. Sato, N. Nakajima, K. Ichiguchi, P. Merkel, J. Nührenberg, U. Schwenn, H. Gardner, A. Bhattacharjee and C.C.Hegna, *Behavior of Magnetic Islands in 3D MHD Equilibria of Helical Devices*; Sep. 1994 (IAEA-CN-60/D-2-II-4)

NIFS-306 S. Murakami, M. Okamoto, N. Nakajima, K.Y. Watanabe, T. Watari, T. Mutoh, R. Kumazawa and T. Seki, *Monte Carlo Simulation for ICRF Heating in Heliotron/Torsatrons*; Sep. 1994 (IAEA-CN-60/D-P-I-14)

NIFS-307 Y. Takeiri, A. Ando, O. Kaneko, Y. Oka, K. Tsumori, R. Akiyama, E. Asano, T. Kawamoto, T. Kuroda, M. Tanaka and H. Kawakami,
Development of an Intense Negative Hydrogen Ion Source with a Wide-Range of External Magnetic Filter Field; Sep. 1994

NIFS-308 T. Hayashi, T. Sato, H.J. Gardner and J.D. Meiss,
Evolution of Magnetic Islands in a Heliac; Sep. 1994

NIFS-309 H. Amo, T. Sato and A. Kageyama,
Intermittent Energy Bursts and Recurrent Topological Change of a Twisting Magnetic Flux Tube; Sep.1994

NIFS-310 T. Yamagishi and H. Sanuki,
Effect of Anomalous Plasma Transport on Radial Electric Field in Torsatron/Heliotron; Sep. 1994

NIFS-311 K. Watanabe, T. Sato and Y. Nakayama,
Current-profile Flattening and Hot Core Shift due to the Nonlinear Development of Resistive Kink Mode; Oct. 1994

NIFS-312 M. Salimullah, B. Dasgupta, K. Watanabe and T. Sato,
Modification and Damping of Alfvén Waves in a Magnetized Dusty Plasma; Oct. 1994

NIFS-313 K. Ida, Y. Miura, S -I. Itoh, J.V. Hofmann, A. Fukuyama, S. Hidekuma, H. Sanuki, H. Idei, H. Yamada, H. Iguchi, K. Itoh,
Physical Mechanism Determining the Radial Electric Field and its Radial Structure in a Toroidal Plasma; Oct. 1994

NIFS-314 Shao-ping Zhu, R. Horiuchi, T. Sato and The Complexity Simulation Group,
Non-Taylor Magnetohydrodynamic Self-Organization; Oct. 1994

NIFS-315 M. Tanaka,
Collisionless Magnetic Reconnection Associated with Coalescence of Flux Bundles; Nov. 1994

NIFS-316 M. Tanaka,
Macro-EM Particle Simulation Method and A Study of Collisionless Magnetic Reconnection; Nov. 1994

NIFS-317 A. Fujisawa, H. Iguchi, M. Sasao and Y. Hamada,
Second Order Focusing Property of 210° Cylindrical Energy Analyzer; Nov. 1994

NIFS-318 T. Sato and Complexity Simulation Group,
Complexity in Plasma - A Grand View of Self- Organization; Nov. 1994

NIFS-319 Y. Todo, T. Sato, K. Watanabe, T.H. Watanabe and R. Horiuchi,
MHD-Vlasov Simulation of the Toroidal Alfvén Eigenmode; Nov. 1994

NIFS-320 A. Kageyama, T. Sato and The Complexity Simulation Group,
Computer Simulation of a Magnetohydrodynamic Dynamo II: Nov. 1994

NIFS-321 A. Bhattacharjee, T. Hayashi, C.C.Hegna, N. Nakajima and T. Sato,
Theory of Pressure-induced Islands and Self-healing in Three-dimensional Toroidal Magnetohydrodynamic Equilibria; Nov. 1994

NIFS-322 A. Iiyoshi, K. Yamazaki and the LHD Group,
Recent Studies of the Large Helical Device; Nov. 1994

NIFS-323 A. Iiyoshi and K. Yamazaki,
The Next Large Helical Devices; Nov. 1994

NIFS-324 V.D. Pustovitov
Quasisymmetry Equations for Conventional Stellarators; Nov. 1994

NIFS-325 A. Taniike, M. Sasao, Y. Hamada, J. Fujita, M. Wada,
The Energy Broadening Resulting from Electron Stripping Process of a Low Energy Au^- Beam; Dec. 1994

NIFS-326 I. Viniar and S. Sudo,
New Pellet Production and Acceleration Technologies for High Speed Pellet Injection System "HIPEL" in Large Helical Device; Dec. 1994

NIFS-327 Y. Hamada, A. Nishizawa, Y. Kawasumi, K. Kawahata, K. Itoh, A. Ejiri, K. Toi, K. Narihara, K. Sato, T. Seki, H. Iguchi, A. Fujisawa, K. Adachi, S. Hidekuma, S. Hirokura, K. Ida, M. Kojima, J. Koong, R. Kumazawa, H. Kuramoto, R. Liang, T. Minami, H. Sakakita, M. Sasao, K.N. Sato, T. Tsuzuki, J. Xu, I. Yamada, T. Watari,
Fast Potential Change in Sawteeth in JIPP T-IIU Tokamak Plasmas; Dec. 1994

NIFS-328 V.D. Pustovitov,
Effect of Satellite Helical Harmonics on the Stellarator Configuration; Dec. 1994

NIFS-329 K. Itoh, S-I. Itoh and A. Fukuyama,
A Model of Sawtooth Based on the Transport Catastrophe; Dec. 1994

NIFS-330 K. Nagasaki, A. Ejiri,
Launching Conditions for Electron Cyclotron Heating in a Sheared Magnetic Field; Jan. 1995

NIFS-331 T.H. Watanabe, Y. Todo, R. Horiuchi, K. Watanabe, T. Sato,
An Advanced Electrostatic Particle Simulation Algorithm for Implicit Time Integration; Jan. 1995

NIFS-332 N. Bekki and T. Karakisawa,
Bifurcations from Periodic Solution in a Simplified Model of Two-

dimensional Magnetoconvection; Jan. 1995

NIFS-333 K. Itoh, S.-I. Itoh, M. Yagi, A. Fukuyama,
Theory of Anomalous Transport in Reverse Field Pinch; Jan. 1995

NIFS-334 K. Nagasaki, A. Isayama and A. Ejiri
Application of Grating Polarizer to 106.4GHz ECH System on Heliotron-E; Jan. 1995

NIFS-335 H. Takamaru, T. Sato, R. Horiuchi, K. Watanabe and Complexity Simulation Group,
A Self-Consistent Open Boundary Model for Particle Simulation in Plasmas; Feb. 1995

NIFS-336 B.B. Kadomtsev,
Quantum Telegragh : is it possible?; Feb. 1995

NIFS-337 B.B.Kadomtsev,
Ball Lightning as Self-Organization Phenomenon; Feb. 1995

NIFS-338 Y. Takeiri, A. Ando, O. Kaneko, Y. Oka, K. Tsumori, R. Akiyama, E. Asano, T. Kawamoto, M. Tanaka and T. Kuroda,
High-Energy Acceleration of an Intense Negative Ion Beam; Feb. 1995

NIFS-339 K. Toi, T. Morisaki, S. Sakakibara, S. Ohdachi, T.Minami, S. Morita, H. Yamada, K. Tanaka, K. Ida, S. Okamura, A. Ejiri, H. Iguchi, K. Nishimura, K. Matsuoka, A. Ando, J. Xu, I. Yamada, K. Narihara, R. Akiyama, H. Idei, S. Kubo, T. Ozaki, C. Takahashi, K. Tsumori,
H-Mode Study in CHS; Feb. 1995

NIFS-340 T. Okada and H. Tazawa,
Filamentation Instability in a Light Ion Beam-plasma System with External Magnetic Field; Feb. 1995

NIFS-341 T. Watanbe, G. Gnudi,
A New Algorithm for Differential-Algebraic Equations Based on HIDM; Feb. 13, 1995

NIFS-342 Y. Nejoh,
New Stationary Solutions of the Nonlinear Drift Wave Equation; Feb. 1995

NIFS-343 A. Ejiri, S. Sakakibara and K. Kawahata,
Signal Based Mixing Analysis for the Magnetohydrodynamic Mode Reconstruction from Homodyne Microwave Reflectometry; Mar.. 1995

NIFS-344 B.B.Kadomtsev, K. Itoh, S.-I. Itoh
Fast Change in Core Transport after L-H Transition; Mar. 1995